Distinguishing features from outliers in automatic Kriging-based filtering of MBES data: a comparative study

P. Bottelier[1], C. Briese[2], N. Hennis[3], R. Lindenbergh[3] and N. Pfeifer[3]

[1] Fugro Intersite BV
[2] Institute of Photogrammetry, Vienna UT
[3] Delft Institute of Earth Observation and Space Systems, Delft UT

1 Introduction

Multi beam echo sounding (MBES) is the state of the art technique of surveying sea floors. A set of sound signals, a ping, is emitted simultaneously, at distinct angles, towards the sea floor. The time it takes for a signal to travel to the sea floor and back is used, together with the angle of emittance, to determine the position and depth of the point of reflection on the sea floor. MBES surveys produce large data sets. Typically, several measurements are available for every square meter in coastal waters. In case of offshore engineering, often real-time processing of the MBES data is required, for example to verify if a pipeline construction turned out successfully. The processing of MBES consists basically of two steps: outliers should be removed and the data density should be decreased, while maintaining a realistic model of the sea bottom. For this purpose a first automatic filtering and thinning algorithm was designed, based on Kriging. Unfortunately, this algorithm had an important drawback: not only blunders, also points representing pipelines were removed by the algorithm.

As the removal of features like pipelines is highly unwanted, methods for improvement were considered. In this paper we discuss these methods and test them on four different data sets of MBES data containing different configurations of pipelines.

The first new method is an extension of the original algorithm. In the original algorithm, soundings are cross-validated in one specific direction, the so-called ping direction. A 1D covariance function is used by the interpolation method Kriging to predict a depth value that is compared with the measured value. If the difference exceeds a certain test value, the measured depth is considered an outlier. Measurements from pipelines perpendicular to the ping direction are easily considered outliers. We show that by using 2D cross-validation this problem can be partially solved. It should be noted that some of the definitions used in the two approaches discussed so far are not considered standard. But as these definitions are used in the implementation causing the problems that initiated this research, we have chosen to present the original definitions rather than standard methods.

An alternative method, also using the Kriging paradigm, was originally designed for filtering laser altimetry data. This type of data, where the time is measured that an emitted light pulse needs for traveling from the laser sensor, mounted on an aircraft, towards the earth and back, is often used to determine a Digital Elevation Model of the bare earth. But laser points are not only reflected by the bare earth but by trees as well. The `tree points' are filtered away as follows. By using a covariance function with a smoothing effect, an average elevation is determined of all available laser points. Now this average elevation divides the measurements in two groups: points below the average are probably bare earth points, points above it are probably tree points. An iterative version of this algorithm turns out to be very effective. We apply this method on our pipeline data. In the multi beam setting we want to filter the `real' outliers/spikes from the sea bottom data including the pipes.

Finally the results of the methods are compared on the data sets, giving satisfying results in most cases.

2 Multi Beam Echo Sounding

Echo sounding is based on the principle that water is an excellent medium for the transmission of sound waves and that part of a sound pulse will return to its source as an echo. If a pulse is emitted from the bottom of the ship at an angle ψ with the vertical line through the emitter, the depth d and the position y of the sea floor hit by this pulse are determined from $(d, y) = ct(\cos\psi, \sin\psi)/2$ where t denotes the time it takes between the initiation of the sound pulse, traveling with velocity c, and reception of the echo, see also Fig. 1.

As illustrated, a swath MBES system (De Jong *et al.* 2002) transmits an acoustic pulse that resembles a fan. Per pulse transmission a high number of depths is thus generated. A ping contains, by definition, all soundings from one pulse transmission. Transversal to the pings are the beams: a beam consists of all soundings with the same emittance angle ψ, therefore a beam contains exactly one sounding of every ping. By combining the depth d and the position y with the position of the ship, determined real-time by GPS (Global Positioning System) and INS (Inertial Navigation System), one obtains coordinate system referenced xyz-data of the sea floor.

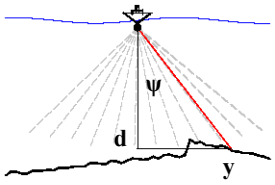

Fig. 1. The multi beam geometry. Shown is one ping of signals

The total list of MBES error sources is extensive. A major error source is wave-induced movement of the ship that can be divided in pitch, roll, heave and heading errors. However, these errors should be eliminated immediately by the INS motion sensors mounted at the ship. Another important error source is the positioning of the ship, done by GPS. The errors we consider however are not the systematic ones, but the real blunders, caused by reflection of the signal on fish or debris, or by occasional electronic errors.

3 Filter methods

All methods we consider are based on the geostatistical interpolation method Kriging (Chilès and Delfiner 1999 and Cressie 1991). Therefore we first recall its basics. The first two filter methods apply Kriging-based cross-validation. In the first case 1D cross-validation is used, in the second 2D. The last, iterative, method uses Kriging to define a smoothed approximation of the sea floor.

3.1 Kriging

Kriging determines weights w_i for the prediction of a depth $\hat{z}_0 = w_1 z_1 + \ldots w_n z_n$ at location p_0, given depth observations $z_1,\ldots,z_n$ at locations $p_1,\ldots,p_n$ and given a covariance function that returns a covariance value as a function of horizontal distance between the observations (isotropic case). First we discuss theoretical and empirical covariance functions, then we show how Kriging uses a covariance function to determine the weights in an optimal way.

The covariance function. The theoretical covariance function or second moment of a stationary random function Z(x) is defined as Cov(s) = E{Z(x)-m}{Z(x+s)-m}, where m=E{Z(x)} denotes the mean or first moment of Z(x). Given some observations a discrete experimental covariance function can be determined by computing experimental covariances between any two observations and by grouping the obtained outcomes according to some distance interval. A continuous covariance function is obtained from the experimental values by fitting them into a covariance model. One can also take a covariance function that is suited to perform some special task. For example, a Gaussian covariance model without nugget effect but with a long range drops relatively slow and therefore has a smoothing effect on the data interpolation.

Ordinary Kriging. Suppose that, as above, we are given height measurements z_1, ..., z_n and want to predict a height $\hat{z}_0 = w_1 z_1 + \ldots w_n z_n$ at position (x_0, y_0). Assume moreover that we are given a covariance function cov(.) producing a covariance value C_{ij} between two positions (x_i, y_i) and (x_j, y_j). The ordinary Kriging system consists of $n+1$ equations:

$$w_1 C_{i1} + w_2 C_{i2} + \ldots + w_n C_{in} + \mu = C_{i0} \quad \text{for all } i = 1, \ldots, n$$
$$w_1 + w_2 + \cdots w_n = 1. \tag{3.1}$$

This implies that the weights can be found by:

$$\begin{pmatrix} w_1 \\ \vdots \\ w_n \\ \mu \end{pmatrix} = \begin{pmatrix} C_{11} & \cdots & C_{1n} & 1 \\ \vdots & \ddots & \vdots & \vdots \\ C_{n1} & \cdots & C_{nn} & 1 \\ 1 & \cdots & 1 & 0 \end{pmatrix}^{-1} \cdot \begin{pmatrix} C_{10} \\ \vdots \\ C_{n0} \\ 1 \end{pmatrix}. \tag{3.2}$$

The μ is a so-called Lagrange multiplier and is an extra variable added to make the system solvable. The ordinary Kriging system is obtained within a *random function model*. This means that with every position a random variable is associated. In the case of ordinary Kriging it is assumed that the expected height is independent of the location and that the mean of the heights is unknown. Ordinary Kriging aims at optimizing two parameters and this optimization results in Equations (3.1) and (3.2).

First of all the expected error $r_0 = \hat{z}_0 - z_0$ in the height prediction should be *unbiased*. It can be shown that this condition $E\{r_0\} = 0$ leads to the equation $w_1 + \ldots + w_n = 1$. The other aim is to minimize the error variance $\mathrm{Var}\{r_0\}$. Looking for the *best* solution for the weights under this condition gives the other Ordinary Kriging equations. Moreover, one obtains a formula for the error variance $\sigma^2_{\text{prediction}} = \mathrm{Var}\{r_0\}$:

$$\sigma^2_{\text{prediction}} = \sigma^2 - \sum_{i=1}^{n} w_i C_{i0} - \mu \tag{3.3}$$

As the predicted height $\hat{z}_0 = w_1 z_1 + \cdots + w_n z_n$ forms a *linear* combination of the measured heights, it is by now clear why Ordinary Kriging is often called BLUP, Best Linear Unbiased Prediction.

3.2 1D cross validation

The first method we discuss was developed, see (Bottelier *et al.* 2000), as part of a data thinning algorithm. Given one ping of MBES data, outliers are eliminated in two steps. In a first step, all blunders, defined as soundings above a certain minimal depth and below some maximal depth, are eliminated. These two threshold values are based on a priori depth information on the surveyed area.

The second step is a cross validation step: a depth value $\hat{z}_{(x,y)}$ is predicted for every sounding location (x, y). This prediction $\hat{z}$ is compared to the actual measurement $z_{(x,y)}$. If the difference between the predicted and measured depth, relative to the standard deviation, is tested too big, the sounding is rejected.

Predicting the depth value, 1D case. The prediction of the depth values is done ping-wise by means of Kriging using a covariance function based on the soundings in the ping. For this purpose first an experimental, discrete covariance function dcov(B_k) is determined for every ping. A bin width $B=\sum_{i=1}^{n-1}\|p_i - p_{i+1}\|/(n+1)$ is defined as the average horizontal separation distance between consecutive soundings in the ping. The bin B_k consist of all pairs of soundings $\{p_i, p_j\}$ s.t.

$$(k-\tfrac{1}{2})B < \|p_i - p_j\| \le (k+\tfrac{1}{2})B \tag{3.4}$$

The experimental covariance function used in this approach is defined by the following rarely used expression.

$$\begin{aligned} C_0 &= \frac{1}{n}\sum_{i=1}^{n}(z_i-\bar{z})^2 \\ \mathrm{dcov}(\mathrm{B_k}) &= \frac{1}{2\,|B_k|}\sum_{\{i,j\}\in B_k}\frac{(z_i-\bar{z})(z_j-\bar{z})}{(z_i-\bar{z})^2+(z_j-\bar{z})^2}\,C_0, \quad k=1..K \end{aligned} \tag{3.5}$$

To decrease the irregular tendency, this empirical covariance function is smoothed with a moving average of five points. From this smoothed function the distance d of the first zero crossing, and the correlation length ξ, that is, the distance at which the covariance value is dropped, for the first time, to half of the value at distance zero, is determined. The curvature κ at the origin is defined as $\kappa = (\log 0.3149)/\log(\xi/d)$. These parameters, see also (Moritz, 1980), are used to fix the following rarely used analytical hole-effect model, (Kitanidis 1997):

$$\mathrm{cov}(s) = C_0\,(1-f)^{\kappa}\exp(-f^{\kappa}) \quad \text{where} \quad f = s/d \quad \text{and} \quad s,d > 0. \tag{3.6}$$

Using this covariance function, a predicted value $\hat{z}_{(x,y)}$ is determined for each measurement position (x, y) in the ping. Here, only the two neighboring soundings on the left and on the right of the sounding to cross validate are used in the interpolation. Note that from the Kriging we obtain $\sigma_{\mathrm{prediction}}$ as well.

Testing the prediction. The last step is to compare the predicted value $\hat{z}_{(x,y)}$ to the measured value $z_{(x,y)}$. This is not done directly, but, again, the variability of the measurements is taken into account. This variability is split in two components. One component is the measurement noise σ_{noise}, that is included to prevent that an observation is marked an outlier just because of random errors. As an indication of the measurement noise, a percentage of 90% of the root of the difference between the first two experimental covariance values is taken, that is $\sigma_{noise}=0.90\sqrt{C_0 - \mathrm{dcov}(B_1)}$ .The other component is the prediction standard error $\sigma_{\mathrm{prediction}}$ This leads to the following test:

$$\frac{\left|z_{(x,y)} - \hat{z}_{(x,y)}\right|}{\sqrt{\sigma^2_{\mathrm{noise}} + \sigma^2_{\mathrm{prediction}}}} > C_1 \tag{3.7}$$

If the test value C_1 is exceeded, the measurement is considered an outlier and removed. Here it is assumed that the depth data are normally distributed. The test value C_1 is based on a 5% confidence level, yielding a critical level of $C_1 = 1.96$. For normally distributed data this confidence level implies that 5% of the measurements are expected to be tested as outlier.

3.3 2D cross validation

The main difference with the 1D cross validation method is that in the 2D method not only soundings in the current ping are used for determining a covariance function and for the actual cross validation. Instead of one ping, a data set of at least three pings and three beams is considered. Again, first the gross blunders are eliminated by thresholding.

Selecting Neighboring points: The experimental covariance function is determined in basically the same way. All data in the data set, consisting of different beams and pings, are used for determining the experimental covariance function. The same analytic covariance function model is fitted on the experimental covariance data as above.

Since the purpose of this algorithm is to cross validate in two directions, mandatory neighbors in both different pings and different beams are included in the Kriging prediction. Including the mandatory neighbors, a fixed number of e.g. eight closest neighbors is used in the cross validation.

The soundings are tested in a specific order, following the ping and beam indices. If a sounding is considered an outlier it is removed from the list of observations and it will not participate in the testing of the following soundings. It did however participate in the testing of some soundings previous to its own testing. Therefore the tests can not considered to be independent.

3.4 Robust Interpolation

Like the cross validation techniques described in the previous sections, the robust interpolation is a method to filter outliers from a point set describing a surface, see also (Kraus and Pfeifer 1998, Pfeifer *et al.* 2001). One problem with the techniques used so far is that the residuals have quadratic impact on the error variance and ordinary Kriging aims at minimizing the squares of this variance. One way of decreasing the impact of outliers is to minimize another sum of discrepancies function, e.g. a function that is more close to the L_1- norm as in that case the influence of residuals only would increase linearly with their size. Such minimization can be performed by changing the weights of the observations in an iterative way, by giving suspicious observations less and less influence during the iterations. This technique is known in the literature as the `robust approach', (Kraus 1997, Rottensteiner 2001). The residuals analyzed in our case are the differences between the observations and a surface. This surface changes during every iteration

and is obtained by a slightly adapted version of ordinary Kriging that incorporates the residual weights returned by the residual weight function.

The residual weight function. The basic idea of this approach is to give less influence to soundings that are likely to be erroneous. How `good' the *i*-th sounding is considered after the *k*-th iteration, depends on the residual $r_i^k = z_i - \hat{z}_i^k$ between the observation z_i and the estimation $\hat{z}_i^k$ after the *k*-th iteration. That is, the residuals r_i^k are the input of the residual weight function *q(r)* given by

$$\text{q: } \mathbf{R} \rightarrow [0,1], \qquad \text{q(r)} = \frac{1}{1+(a\,|\,r\,|)^b}. \tag{3.8}$$

So, the individual residual weight q_i^{k+1} for the next, the *(k+1)*-th, iteration is determined as $q_i^{k+1} = q(r_i^{k+1})$. If, however, a residual weight q_i^{k+1} is smaller then a certain threshold value $0 \le \varepsilon < 1$, the observation z_i is marked as erroneous and removed from the set of observations. The shape of the residual weight function is described by the half-width *1/a* and the slope *4/ab* at the half-width point *(1/a, q(1/a))*. Before the first estimation step all residual weights are initialized to *1*, that is, $r_i^0 = 1$ for all *i*.

The covariance model. In order for the residual weight function to work properly, the predictions should be on a rather smooth surface that runs on an averaging way between the `real' observations and the `erroneous' observations. Such surface can be obtained by combining two effects. One is to omit the nugget effect in the proximity vector $\boldsymbol{c}$ of covariances with the interpolation position, compare Equation 3.2. The other is to use a covariance model with an almost horizontal slope near the origin and with a not too small range. The covariance function for the area under study follows the Gaussian model, (Wackernagel, 1998), with the same correlation length ξ, see Subsection 3.2 everywhere:

$$\text{cov}(s) = C_0 \exp\left(-\left(\frac{s \ln 2}{\xi}\right)^2\right);\ s > 0 \tag{3.9}$$

Here, C_0 denotes the maximum of the covariance function, defined by $C_0 = \sum_i (z_i - z)^2 - \sigma^2$, and *s* the horizontal distance between observations. The measurement accuracy is denoted by σ. To assume isotropy in the data sets considered seems justified by the satisfying results obtained by this method. Note that cov*(s)* is the same in every iteration, for *s>0*. So, the off-diagonal elements of the variance-covariance matrix are given by $C_{ij} = \text{cov}(\,||\, p_i - p_j \,||\,)$, where p_i and p_j denote the positions of the observations z_i and z_j.

The interpolation step. The diagonal elements of the variance-covariance matrix however are iteration step, k, dependent and are given by $C_{ii}^{k} = C_0 + \sigma^2 / q_i^k$. They contain a nugget effect σ^2 / q_i^k that incorporates the individual residual weight q_i^k. This ensures that suspicious observations have less influence in the interpolation. The nugget effect is omitted in the proximity vector $\boldsymbol{c} = C_{i0}$ of covariances with the interpolation position, so $C_{i0} = \text{cov}\,(\,||\,p_i - p_0\,||\,)$ if $p_i \neq p_0$ and $C_{i0} = C_0$ if $p_i = p_0$. This is a well-known technique to filter short-scale signals and is known as filtering, (Goovaerts 1997). By now all entries of the Ordinary Kriging system of Equation 3.2 are given and the Kriging weights for the next iteration can be determined, resulting in new residuals between the observations and new estimations and thereby in new residual weights. Finally, at every iteration, observations with a residual smaller than the threshold value ε are marked as outlier and removed. This can simply be done by wiping out the row and column corresponding to the outlying observation. The algorithm terminates after a fixed number of iterations, or after all residuals drop below some critical value. If, ideally, all residual weights are close to one, the distances from the observations to the interpolated surface will be in the order of the measurement accuracy σ.

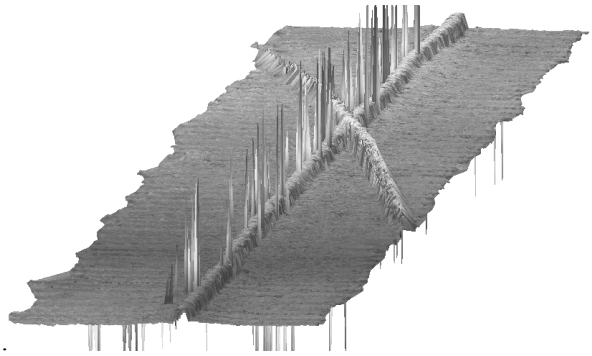

Fig. 2. Data set 1 before processing.

4 Filtering the data sets

For testing the different methods, four data sets are used. We will concentrate on the first however, see Fig. 2., obtained by a multi beam system mounted on a ROV, a Remotely Operated Vehicle, operating at about 15 m above the sea floor. This data set has been acquired using a Reson Seabat 9001 multi beam system. This system has 60 beams and a ping rate of 7 pings a second. The average depth is around 145 meter and the distance between consecutive pings is approximately 0.03 m and the approximate distance between two adjoining beams is 0.1 m.

The second data set has an average depth of approximately 13 meter in the first half and then 23 meter in the second half. The approximate distance between consecutive pings is 0.13 m and between two adjoining beams 0.45 m. This data set does not cover pipelines but represents a short steep sloop.

The third and fourth data set have an average depth of around 300 meters and approximate distance of 0.12-0.14 m between consecutive pings and 0.19-0.24 m between adjoining beams. In both data sets a pipe and some templates are present.

Parameter choices for the different methods: In the 2D method it was possible to vary the number of pings processed at once and to select the number of neighbors. The data presented here were obtained by processing 10 pings at a time while 8 neighbors were used for the cross validation. Although the exact numbers change, similar results were obtained with different parameter choices.

The robust method was run with a maximum of seven iterations. The measurement accuracy was σ=10 cm, the half-width was set on $1/a=2\sigma$, while b=2.

4.1 The results

Table 1. Numbers and percentages of removed outliers by the different methods.

	1D method	2D method	Robust method
MBES 1	104 040	111 476	111 476
# outliers	3 149	1 394	193
% outliers	3.03	1.25	0.17
MBES 2	125 245	130 641	130 641
# outliers	3 853	1 746	1 407
% outliers	3.08	1.34	1.08
MBES 3	297 958	303 014	303 014
# outliers	4 364	3 084	256
% outliers	1.46	1.02	0.08
MBES 4	215 557	219 217	219 217
# outliers	1 955	3 479	1 154
% outliers	0.91	1.59	0.53

Unfortunately it is not very clear what distinguishes good from bad soundings, or, which soundings should be removed. The methods discussed above all divide the soundings objectively in one of these two categories. In most cases it is, subjectively, clear, by a simple visualization, if a wrong decision is made. Often (Teunissen 2000) the following two types of wrong decisions are distinguished: on one hand a Type I error: a sounding is rejected, although it is correct and on the other hand a Type II error: a sounding is accepted, although it is wrong

In Table 1 the numbers of outliers removed are given. Clearly, the 1D method finds a lot of `outliers'. As the 1D method is designed as a data thinning procedure this is an essential part of the algorithm. In the case of data set 1 however, a lot of type I errors are made, due to the presence of the pipelines. This was the reason to

consider alternative methods. In general the 2D method removes fewer soundings, but as we will see later, still type I errors are made. Based on visual inspection, we conclude that the robust method removes the smallest number of points and seems to perform the best, by minimizing both the number of type I and type II errors.

Results of 1D method. In Fig. 3 the results of the 1D algorithm applied on the first data set are shown. On the left a Digital Elevation Model (DEM) of the accepted soundings is given while on the right a top view is given of the accepted soundings in gray and the rejected soundings, in black. The DEM still contains spikes, while the top view shows that a lot of `outliers' were found on the diagonal pipe. The DEM of the data set before processing however, see Fig. 2, shows no outliers on the diagonal pipe. From this visual inspection we conclude that some outliers were not found while many `good' points were rejected by the algorithm.

Results of 2D method. Fig. 4 shows the results of the 2D algorithm on the first data set. In this case no more clear spikes are present in the Digital Elevation Model on the left. The number of soundings marked as outliers is much lower than in the 1D case as can be seen in the top view image on the right. Still many soundings are rejected as outlier situated near the diagonal pipe. We conclude that most of the reported outliers for the 1D and 2D approach are removed unwantedly and should be considered type I errors.

Results of the robust method. In Fig. 5 an overview is given of the accepted soundings, again in gray, and the rejected ones, in black. The digital elevation model of the accepted soundings is not given in this case, as it is similar to the one shown in Fig. 4: no obvious spikes are left after applying the robust method. The robust method only reports a small number of outliers, about one tenth of the number returned by the 2D method, while all spikes seem to be removed. Moreover, only a few `outliers' were found on the diagonal pipe. Still these `outliers' seems to be type I errors, indicating that even the robust method has some problems with the pipes.

5 Conclusions

Both the 1D and 2D method are forced to filter away good points by the 5% confidence level. If the confidence level drops, the number of Type II errors will however increase. Before applying these methods one should have a rough idea on the expected number of outliers. Here, the analysis of Receiver Operating Characteristic Curves could help in future to visualize how the proportion of false alarms increases as the confidence level increases. It should also be considered what the local impact (near features) of a globally set confidence level is.

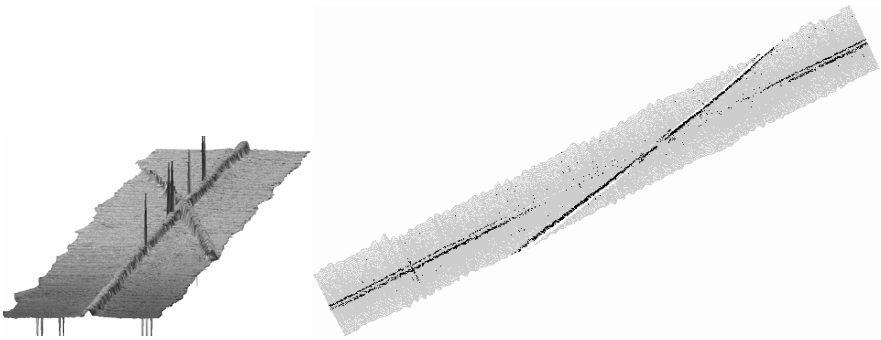

Fig. 3. Data set 1 processed by the 1D method: on the left the DEM of the accepted soundings, on the right a top view of the accepted soundings, gray, and the rejected, black.

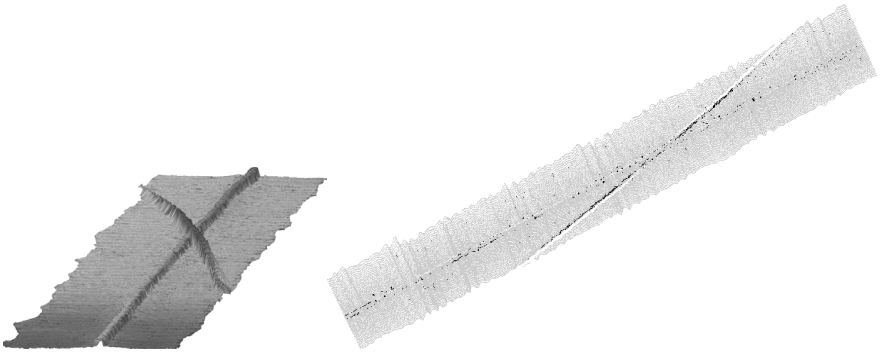

Fig. 4. Data set 1 after processing with the 2D method.

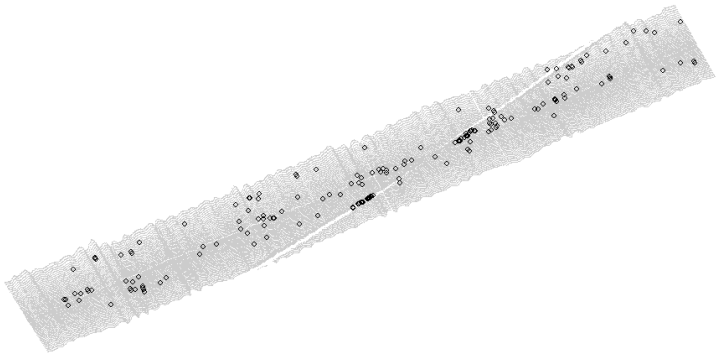

Fig. 5. Accepted and rejected soundings of Data set 1, as found by the Robust method.

In the 2D method, forced including of soundings of different pings is applied. But these included soundings do not get automatically a relevant interpolation weight: for the first two data sets, the ratio of ping width versus beam width is 1:3. Therefore the 2D method is to some extent still a `1D method'.

Both the 2D method and the robust method can be very time inefficient if implemented without consideration. The parameters of the covariance function should preferably be determined in a heuristic way while the number of soundings processed at once should not become too big. The number of soundings included in the Kriging system should be strongly limited while in selecting small number of neighbors one could try to use the structure of the data file.

Analyzing and comparing the results of the different methods is difficult, as it is uncertain which points are truth `ground points' and which points are outliers. A similar comparison on small simulated datasets could be helpful. This would also make it possible to analyze what kind and relative size of features will cause problems for the different methods.

Acknowledgments

The Delft UT Research Theme Earth is thanked for financial support enabling the useful visit of C. Briese to the Delft University of Technology. Fugro Intersite BV and namely C. de Jong are thanked for raising the problem, hosting Natasha Hennis and for the data sets. Finally the reviewers are thanked for their many helpful comments and suggestions.

References

Bottelier P, Haagmans R, Kinneging N (2000) Fast reduction of high density multibeam echosounder data for near real-time applications. The Hydrographic Journal, 98:23-28

Chilès JP, Delfiner P (1999) Geostatistics: modeling spatial uncertainty. Wiley, New York

Cressie NAC (1991). Statistics for Spatial Data, Wiley, New York

de Jong CD, Lachapelle G, Skone S, and Elema IA (2002) Hydrography. Delft University Press, Delft

Goovaerts P (1997) Geostatistics for Natural Resources Evaluation. Oxford University Press, Oxford

Kitanidis P (1997) Introduction to Geostatistics. Cambridge University Press. Cambridge.

Kraus K (1997) Photogrammetry - Advanced Methods and Applications. Dümmler, Bonn

Kraus K, Pfeifer N (1998) Determination of terrain models in wooded areas with airborne laser scanner data. ISPRS Journal of Photogrammetry and Remote Sensing 53:193-203

Moritz, H (1980) Advanced Physical Geodesy. Abacus Press, Tunbridge Wells

Pfeifer N, Stadler P, Briese C (2001) Derivation of digital terrain models in the SCOP++ environment. OEEPE Workshop on Airborne Laserscanning and Interferometric SAR for Digital Elevation Models, OEEPE Publication 40, Stockholm

Rottensteiner F (2001) Semi-automatic extraction of buildings based on hybrid adjustment using 3D surface models and management of building data in a TIS. PhD Thesis, Vienna University of Technology

Teunissen PJG (2000) Testing theory; an introduction. Delft University Press, Delft

Wackernagel H (1998) Multivariate Geostatistics, 2nd edition, Springer, Berlin